OXFORD
SOT | Society of Toxicology
www.toxsci.oxfordjournals.org

TOXICOLOGICAL SCIENCES, 141(1), 2014, 300–313

doi: 10.1093/toxsci/kfu127
Advance Access Publication Date: June 27, 2014

Intracellular Generation of ROS by 3,5-Dimethylaminophenol: Persistence, Cellular Response, and Impact of Molecular Toxicity

Ming-Wei Chao*,†,[1], Pinar Erkekoglu†,‡, Chia-Yi Tseng§, Wenjie Ye†, Laura J. Trudel†, Paul L. Skipper†, Steven R. Tannenbaum†, and Gerald N. Wogan†

*Department of Bioscience Technology, Chung Yuan Christian University, Chungli City, Taoyuan 32023, Taiwan, †Department of Biological Engineering, Massachusetts Institute of Technology, Cambridge, Massachusetts 02139, ‡Department of Toxicology, Faculty of Pharmacy, Hacettepe University, Sihhiye-Ankara, Turkey and §Department of Biomedical Engineering, Chung Yuan Christian University, Chungli City, Taoyuan 32023, Taiwan

[1]To whom correspondence should be addressed at Department of Bioscience and Technology, College of Science, Chung Yuan Christian University, 200 Chung Pei Road, Chungli City, Taoyuan 32023, Taiwan. Fax: +886-3-265-3599. E-mail: chao@cycu.edu.tw.

ABSTRACT

Epidemiological studies have demonstrated extensive human exposure to the monocyclic aromatic amines, particularly to 3,5-dimethylaniline, and found an association between exposure to these compounds and risk for bladder cancer. Little is known about molecular mechanisms that might lead to the observed risk. We previously suggested that the hydroxylated 3,5-dimethylaniline metabolite, 3,5-dimethylaminophenol (3,5-DMAP), played a central role in effecting genetic change through the generation of reactive oxygen species (ROS) in a redox cycle with 3,5-dimethylquinoneimine. Experiments here characterize ROS generation by 3,5-DMAP exposure in nucleotide repair-proficient and -deficient Chinese hamster ovary cells as a function of time. Besides, various cellular responses discussed herein indicate that ROS production is the principal cause of cytotoxicity. Fluorescence microscopy of cells exposed to 3,5-DMAP confirmed that ROS production occurs in the nuclear compartment, as suggested by a previous study demonstrating covalent linkage between 3,5-DMAP and histones. 3,5-DMAP was also compared with 3,5-dimethylhydroquinone to determine whether substitution of one of the phenolic hydroxyl groups by an amino group had a significant effect on some of the investigated parameters. The comparatively much longer duration of observable ROS produced by 3,5-DMAP (7 vs. 1 day) provides further evidence that 3,5-DMAP becomes embedded in the cellular matrix in a form capable of continued redox cycling. 3,5-DMAP also induced dose-dependent increase of H_2O_2 and ·OH, which were determined as the major free radicals contributing to the cytotoxicity and apoptosis mediated via caspase-3 activation. Overall, this study provides insight into the progression of alkylaniline-induced toxicity.

Key words: reactive oxygen species; dimethylaminophenol; quinone imine; hydroquinone; apoptosis

Table of Content Graphics: A picture of monocyclic aromatic amine (MAA) genotoxicity that emerges is one of the transamination to lysine residues in proteins followed by long-term redox cycling that exposes DNA to reactive oxygen species (ROS).

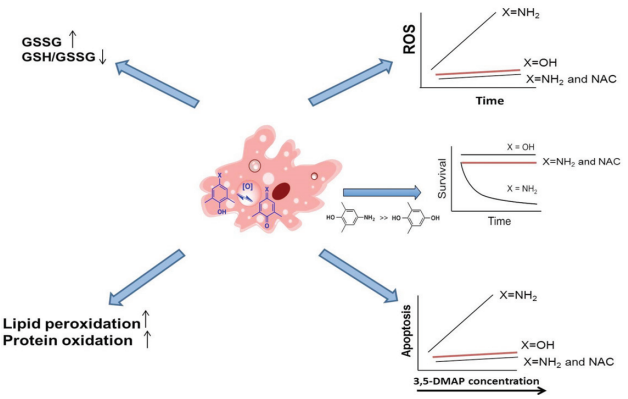

Although some aromatic amines, e.g., 4-aminobiphenyl, are well-documented risk factors for bladder cancer (Martone *et al.*, 1998; Van Hemelrijck *et al.*, 2009), evidence linking exposure to MAAs, particularly alkylanilines, to this type of cancer is less extensive (Skipper *et al.*, 2010). 2,6-dimethylaniline (2,6-DMA), a well-known alkylaniline, has been classified as a possible human carcinogen (Group 2B) by the International Agency on Research on Cancer on the basis of its nasopharyngeal carcinogenicity in rats (Short *et al.*, 1989). In humans, exposure to 2,6-DMA, 3,5-dimethylaniline (3,5-DMA), and 3-ethylaniline has each been associated with increased bladder cancer risk in nonsmokers residing in Los Angeles county (Gan *et al.*, 2004). On the other hand, cigarette smoke (CS) is an outstanding source of free radicals and ROS and several alkylanilines are present in CS (Micale *et al.*, 2013). In experimental animals, these compounds were metabolically activated to electrophilic derivatives and apparently formed DNA adducts in the urinary bladder (Skipper *et al.*, 2006). Presumptive adduct levels were highest in tissues of animals dosed with 3,5-DMA and lowest in those given 3-ethylaniline. These *in vivo* experiments generated carcinogen binding indices (CBIs) consistent with the hypothesis that DNA adducts formed by 3,5-DMA might account for its presumptive genotoxic activity. CBIs for the other two amines were indicative of weak carcinogenicity. Cui *et al.* (2007) provided *in vitro* chemical support for a mechanism of 3,5-DMA carcinogenicity based on *N*-hydroxylation and the intermediacy of a nitrenium ion in the formation of DNA adducts (Cui *et al.*, 2007).

Oxidative stress can be defined as the imbalance between cellular oxidant species production and antioxidant capability (Mates *et al.*, 2008). ROS can be produced during normal cellular function or can emerge after exposure to environmental chemicals. ROS are very transient, and due to their high chemical reactivity they lead to lipid peroxidation (LP) and massive protein oxidation and degradation (Hengstler and Bolt, 2008; Mates *et al.*, 2012). Superoxide anion ($O_2\cdot^-$) and hydroxyl radical (·OH) are recognized as inducers of mutagenesis by direct chemical reaction with DNA. Additionally, hydrogen peroxide (H_2O_2) can also induce mutagenesis and DNA damage (Maynard *et al.*, 2009). ROS are also known to induce secondary effects such as signal transduction (Suzuki *et al.*, 1997), chemotaxis (Moslen, 1994), apoptosis (Breimer, 1990; Moreno-Manzano *et al.*, 2000), and necrosis (Mates *et al.*, 2008), can function as secondary messengers

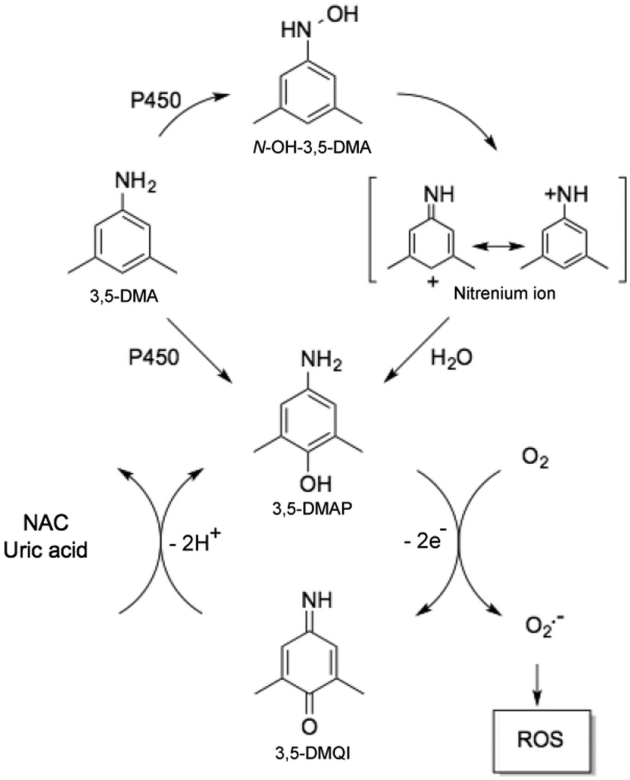

FIG. 1. Pathway for the production of ROS by 3,5-DMAP following exposure of a metabolically competent biological system to 3,5-dimethylaniline. 3,5-DMA: 3,5-dimethylaniline; N-OH-3,5-DMA: N-hydroxyl-3,5-dimethylaniline; 3,5-DMAP: 3,5-dimethylaminophenol; 3,5-DMQI: 3,5-dimethylquinone imine; CYP450: cytochrome P450 enzymes; NAC: N-acetyl cysteine. CYP450s convert 3,5-DMA to N-OH-3,5-DMA and 3,5-DMAP. The N-hydroxylamine undergoes N-O-bond heterolysis, catalyzed by acyl- or sulfo-transferase activity that forms an unstable N-O- ester. The intermediate nitrenium ion formed reacts with a DNA base to produce a mutagenic adduct. The 3,5-DMAP produced by P450-catalyzed hydroxylation of the aniline or by nucleophilic attack of H2O on the appropriate resonance form of the nitrenium ion is oxidized to its quinone imine form. The electrophilic 3,5-DMQI undergoes redox cycling to generate ROS that results in genotoxic and cytotoxic activities. ROS scavengers, NAC, and uric acid are able to attenuate the cycling pathway between 3,5-DMAP and 3,5-DMQI.

(Natoli *et al.*, 1997; Schreck *et al.*, 1991), and may cause induction of cell proliferation and carcinogenesis (Mates *et al.*, 2008). More recently, we have conducted experiments using Chinese hamster ovary (CHO) cells. These studies revealed an alternative mechanism for genotoxic activity of 2,6-DMA and 3,5-DMA, namely, the production of ROS by phenolic metabolites of the alkylanilines. This finding also suggests a greater role for ROS in alkylaniline toxicity than for formation of covalent DNA adducts (Chao *et al.*, 2012). Previous investigations have also shown that the other MAAs, namely, aniline (Bomhard and Herbold, 2005; Ma *et al.*, 2008; Tao *et al.*, 2013), toluidine (Pagoria and Geurtsen, 2005), 2,4,6-trimethylaniline (Kugler-Steigmeier *et al.*, 1989), and anisidine cause free radical-induced cytotoxicity (Stiborova *et al.*, 2002).

As argued previously (Chao *et al.*, 2012), the mechanism, by which the alkylanilines 2,6-DMA and 3,5-DMA would generate ROS *in vivo*, involves initial oxidative metabolism to an aminophenol, which then can cycle through the corresponding quinone imine structure. The essential features of this process are outlined in Figure 1. ROS have been implicated in the redox cycling pathway of quinone derivatives

(Barreto *et al.*, 2009; Bolton *et al.*, 2000). Metabolites including semiquinone or hydroquinone have well-documented abilities to induce oxidative stress and cause oxidative and alkylation damage to cellular DNA, proteins, and lipids (Bolton *et al.*, 2000; Hiraku and Kawanishi, 1996; Luo *et al.*, 2008). The multiple Michael addition product 2,3,5-tris-(glutathion-S-yl)hydroquinone is also a highly effective generator of ROS (Hill *et al.*, 1994). The aminophenol/quinone imine couple differs from the hydroquinone/quinone couple only in the substitution of one nitrogen atom for an oxygen atom and thus might be expected to exhibit very similar redox activity. Our previous work also suggested this phenomenon (Chao *et al.*, 2012). We therefore undertook the present experiments to explore in greater detail intracellular production of ROS by an aminophenol in CHO cells and its sequential cytotoxicity effects and to compare that aminophenol with its hydroquinone congener 3,5-dimethylhydroquinone. Several antioxidants, particularly N-acetylcysteine (NAC), were also tested against the oxidative potential of 3,5-dimethylaminophenol (3,5-DMAP).

MATERIALS AND METHODS

Chemicals. N-hydroxyl-3,5-dimethylaniline (NOH-3,5-DMA) and 3,5-DMAP were synthesized with the methods described previously (Chao *et al.*, 2012). The following were purchased from various sources as indicated: dimethyl sulfoxide (DMSO), sulfanilic acid, ascorbic acid, 3,5-dimethylaniline (3,5-DMA), 8-azaadenine, NAC, uric acid, ascorbate, and Tiron from Sigma-Aldrich (St. Louis, MO); 2,6-dimethylhydroquinone (DMHQ) from TCI America (Portland, OR); and bovine erythrocyte superoxide dismutase (SOD, 5000 U/mg) and beef liver catalase (CAT, 65000 U/mg) from Roche Diagnostics (Indianapolis, IN). Stock solutions of all compounds used in cell experiments were freshly prepared in Hank's buffered saline solution (HBSS) except for 3,5-DMAP and 2,6-DMHQ, which were dissolved in DMSO. The primary antibodies of pro-caspase and pro-poly(ADP-ribose)polymerase (pro-PARP) were obtained from Abcam (Cambridge, MA). Secondary goat anti-mouse IgG or anti-rabbit IgG conjugated with horse radish peroxidase (HRP) was purchased from Jackson ImmunoResearch (West Grove, PA). 3,5-DMAP was synthesized from 2,6-dimethylphenol as described for the isomeric 2,6-DMAP (Gan *et al.*, 2001). Briefly, the phenol was coupled with diazotized sulfanilic acid to form 4′-hydroxy-3′,5′-dimethylazobenzene-4-sulfonic acid. 3,5-DMAP was obtained by reduction of the product with $Na_2S_2O_4$. The yield of the final product was 82%. *Caution*: 3,5-DMAP is toxic, mutagenic, and possibly carcinogenic. This compound should be handled using appropriate precautions.

Cell culture. Nuclear excision repair (NER)-proficient AA8 and NER-deficient UV5 cells developed by Thompson *et al.* (1980) were obtained from the American Type Culture Collection (Rockville, MD). Cells were grown in Eagle minimum essential medium (alpha modification M4526, Sigma), supplemented with 10% fetal bovine serum (Atlanta Biologics, Norcross, GA), 200-mM L-glutamine, 100-units/ml penicillin, and 100-units/ml streptomycin (Lonza, Walkersville, MD) in a 5% CO_2 atmosphere at 37°C.

Determination of cytotoxicity. Cytotoxicity of 3,5-DMAP and 3,5-DMHQ in the presence or absence of putative radical scavengers was determined by the 2-(4-iodophenyl)-3-(4-nitrophenyl)-5-(2,4-disulfophenyl)-2H-tetrazolium, monosodium salt (WST) assay (Cell Proliferation Reagent WST-1 kit, Roche Applied Science, Indianapolis, IN). The assay kit measures mitochondrial enzyme activity via reductive conversion of the tetrazolium salt WST-1 to a soluble formazan dye. Cytotoxicity was determined 24 h after treatment. Cells were washed with PBS and suspended in 1-ml fresh medium, and 10 μl aliquots were pipetted into each well of 96-well plates. A mixture of 10 μl kit reagent plus 90 μl fresh medium was added to each well, after which the plate was incubated at 37°C for 1 h in the dark. A μQuant micro-reader (Biotek Instruments Inc., Winooski, VT) was used to quantify the formazan product (A_{495}). Values were normalized and expressed as percentage of the controls.

Quantification and imaging of intracellular ROS generation. Cells were treated with 3,5-DMAP in the presence or absence of NAC (5 mM), ascorbate (50 mg/ml), and with or without ROS scavengers for 1 h, then washed twice with serum-free medium. After addition of fresh medium, cells were incubated at 37°C for 0, 1, 3, 5 h, or 7 days, then washed with PBS and suspended in serum-free medium. To quantify ROS levels, aliquots of 100-μl cell suspensions were pipetted into each well of 96-well plates and each was mixed with 10 μl HBSS containing 5-(and-6)-chloromethyl-2′,7′-dichlorodihydro-fluorescein diacetate, acetyl ester (CM-H_2DCFDA) (Molecular Probes/Invitrogen, Eugene, OR) at a final concentration of 25 μM. Fluorescence intensity (at 495-nm excitation and 514-nm emission) was measured with an HTS 7000 Plus Bio Assay micro-reader (Perkin Elmer Life Sciences, Waltham, MA) after incubation for 30 min at 37°C. Levels were normalized to viable cell numbers and are presented as percentage of DMSO control values. Cells producing ROS were imaged by Nikon epifluorescence microscopy at ×400 magnification (excitation at 488 nm, Nikon Microscope) after treatment with the same CM-H_2DCFDA protocol. Nuclei were stained with 1-μg/ml Hoechst 33258 (Molecular Probes/Invitrogen). Cells treated with 0.9% DMSO or 10-mM H_2O_2 were used as negative and positive controls, respectively.

Total protein, cytoplasmic, and nuclear protein extraction. After treatment, cells were collected and extracted with RIPA lysis buffer (25 mM Tris-HCl pH 7.6) containing 150-mM NaCl, 1% NP-40, 1% sodium deoxycholate, 0.1% SDS, 1-mM phenylmethylsulfonyl fluoride, and sodium orthovanadate supplemented with 20 μg/ml protease inhibitor cocktail (Santa Cruz Biotechnology, Santa Cruz, CA) for 30 min on ice, then centrifuged at 10,000 × *g* for 10 min to remove the pellet. Cell suspensions were harvested by centrifuging at 500 × *g* for 5 min, washed by suspension in PBS and re-pelleted by centrifugation at 500 × *g* for 2–3 min. Dry pellet was processed with an NE-PER nuclear and cytoplasmic extraction kit (Thermo Scientific, Waltham, MA) in the presence of the protease inhibitor cocktail. Protein concentration was measured by the bicinchoninic acid method (BCA protein assay, Thermo Scientific).

Glutathione content, glutathione reductase, SOD activity. Total glutathione (total GSH) content of cell extracts was assessed using a kit (CS0260-1KT, Sigma) based on a kinetic assay in which catalytic amounts of GSH caused a continuous reduction of 5,5′-dithiobis-(2-nitrobenzoic) acid (DTNB) at 412 nm (Akerboom and Sies, 1981). For oxidized glutathione (GSSG) determination, reduced glutathione (GSH) was inactivated by addition of 2-vinylpyridine in the presence of triethanolamine. Quantification was achieved by parallel measurements of GSH or GSSG standards, and results were expressed as nmol/mg protein. GR activity was determined with a kit (GRSA-1KT, Sigma-Aldrich) using the rate of DTNB reduction as the measure of enzyme activity at

412 nm and results are expressed as μmol/min/mg protein. The total SOD activity was measured by a "total SOD activity kit" colorimetrically. The activity was determined by using WST-1 that produces a water-soluble formazan dye upon reduction with a $O_2 \cdot^-$ anion. The rate of the reduction WST-1 to WST-1 formazan with $O_2 \cdot^-$ ion was linearly related to the xanthine oxidase activity and was inhibited by SOD (as SOD provided the dismutation of $O_2 \cdot^-$). The 50% inhibitory activity of SOD against $O_2 \cdot^-$ formation (IC_{50}) was determined by this colorimetric method. Because the absorbance at 440 nm was proportional to the amount of $O_2 \cdot^-$ anion, the inhibitory SOD activity was quantified by measuring the decrease in the color development at 440 nm. The results are expressed as μmol/mg protein.

LP and protein oxidation quantification. LP in nuclear and cytoplasmic extracts was quantified measuring the concentration of thiobarbituric acid reactive substance (TBARS) by a spectrofluorometric assay (at excitation 530 nm and emission 550 nm) using a "TBARS assay kit" (Cayman Chemical Company, Ann Arbor, MI) as described by Richard *et al.* (1992). Quantification was achieved by parallel measurements of a standard curve of known TBARS concentrations, and results were expressed as nmol/g protein. The carbonyl groups as the biomarker of protein oxidation were determined by using 2,4-dinitrophenylhydrazine reaction and the amount of protein-hydrazone produced was quantified spectrophotometrically at 360 nm using a "carbonyl assay kit" (Cayman Chemical Company).

Apoptosis measurement. After exposure of 3×10^6 cells in a 100 mm culture dish to a series of doses of 3,5-DMAP in the presence or absence of NAC, cells were harvested by trypsinization and centrifugation, then stained with Annexin V-FITC and propidium iodide according to the ApoAlert Annexin V (Clontech Laboratories, Mountain View, CA) protocol. After 10 min incubation in dark, the cells were analyzed with a Becton Dickinson FACScan equipped with CellQuest software. Cells labeled with Annexin V (early apoptosis) and with both Annexin V and propidium iodide (late apoptosis) were quantified; those treated with DMSO were used as negative controls. The apoptosis level was normalized and presented as the percentage of controls.

Caspase-3 activity. Caspase-3 activity was assessed using the ApoAlter caspase-3 colorimetric assay kit (Clontech Laboratories). Two million cells were plated onto a 100-mm tissue culture dish; after exposure to 3,5-DMAP in the presence or absence of scavengers with various periods, cells were collected and extracted with ice cold cell lysis buffer, and incubated for 10 min on ice. Cellular debris was removed by centrifuging at 16,000 x *g* for 10 min, then 50-μl reagent mixture (2X reaction buffer/DTT mix and 50 μM caspase-3 substrate DEVD-pNA) was applied according to manufacturer's instructions. After 3 h incubation at 37°C, $A_{405\ nm}$ was determined using a μQuant micro-reader (Biotek Instruments, Inc.). Absorbance values were compared with that of DMSO-treated controls and results were expressed as the average fold difference from controls.

Western blot. Cells were collected for the protein extraction after 3,5-DMAP treatment. Protein lysates were separated on NuPAGE precast gels (BioRad), transferred to 0.45 μm nitrocellulose membranes (BioRad), and probed with appropriate dilution of specific primary antibodies (pro-caspase 3 and pro-PARP). Secondary goat anti-mouse IgG or anti-rabbit IgG conjugated with HRP was used and the protein products were visualized on X-ray film using with chemiluminescent reagent containing luminol. Glyceraldehyde 3-phosphate dehydrogenase was used as a loading control.

Measurement of H_2O_2 production and ·OH production. H_2O_2 production of 3,5-DMAP in AA8 and UV5 was assessed using a commercially available Fluoro H_2O_2 Hydrogen Peroxide Assay kit (DAFDA) purchased from Cell Technology, Inc. (Mountain View, CA). The detection kit utilizes a non-fluorescent reagent that can be oxidized by H_2O_2 and produced fluorescent resorufin (excitation at 540 nm), then the amount of H_2O_2 in the cells was determined. Cell density at 1×10^5 cells per well of a 24-well plate was treated with 3,5-DMAP (50 μM) with or without the ROS scavengers for 1 h, then washed twice with fresh serum free medium. The cells were incubated for further 24 h at 37°C with fresh medium prior to the measurement. The fluorescence of samples was read at 540 nm on an HTS 7000 Plus Bio Assay Reader (Perkin Elmer Life Sciences). The amount of H_2O_2 was normalized and assessed by comparison with the negative control. Hydroxyl radical (·OH) was detected by using a fluorescent novel probe dye 3′-(p-hydroxyphenyl) fluorescein (HPF) from Cell Technology, Inc. HPF developed by Setsukinai *et al.* (Setsukinai *et al.*, 2003) are selective dyes for the detection of ·OH. Cells were plated and treated in the same way as H_2O_2 measurement. Twenty-four hour-incubation after treatments, medium was removed and cells were incubated with 5 μM HPF in HBSS for 60 min at 37°C, under limited light conditions. Fluorescence of samples was monitored using an HTS 7000 Plus Bio Assay Reader (Perkin Elmer Life Sciences) at an excitation wavelength of 490 nm and an emission wavelength of 530 nm. Data are normalized and presented as the percentage difference of the negative controls.

Statistics. Experiments were typically performed in triplicate and results are expressed as mean ± SD. The Student's *t*-test was used for statistical analysis of differences.

RESULTS

Cytotoxicity of 3,5-DMA and its Metabolites and Comparison of ROS Production by 3,5-DMAP and 3,5-DMHQ

Studies have indicated that some aromatic amines such as 4-aminobiphenyl are well-documented risk factors for carcinogenesis (Kim and Guengerich, 2005; Skipper *et al.*, 2003, 2010; Tsuneoka *et al.*, 2003), however, it remains unclear about the genotoxicity and potential carcinogenic risk created by 3,5-DMA exposure. We therefore are investigating the cytotoxicity of 3,5-DMA and its metabolites N-OH-3,5-DMA and 3,5-DMAP in nucleotide repair-proficient AA8 and repair-deficient UV5 cells. Figures 2A and 2B show that the parental chemical, 3,5-DMA, as well as the N-OH-3,5-DMA and 3,5-DMAP derivatives all caused dose-dependent decreases in cell survival, but with very different potencies: 3,5-DMAP had the highest potency (IC_{50}: 40 μM); N-OH-DMA intermediate (IC_{50}: 250 μM); and 3,5-DMA lowest (IC_{50}: 1500 μM) in AA8 and UV5 cells. Cytotoxicity and dose response for ROS generation induced by 1 h exposure to the hydroquinone 3,5-DMHQ were determined 0 and 24 h after exposure with results from AA8 cells shown in Figures 2C and 2D. Results from UV5 cells were virtually identical and can be found in the Supplementary information (Supplementary fig. 1). Time points were chosen to enable direct comparison with previously reported data for 3,5-DMAP (Chao *et al.*, 2012), which are also shown. 3,5-DMAP produced readily detectable ROS at concentrations as low as 25 μM and exhibited increased ROS generation at 24 h as compared with 0 h. In contrast, 3,5-DMHQ was

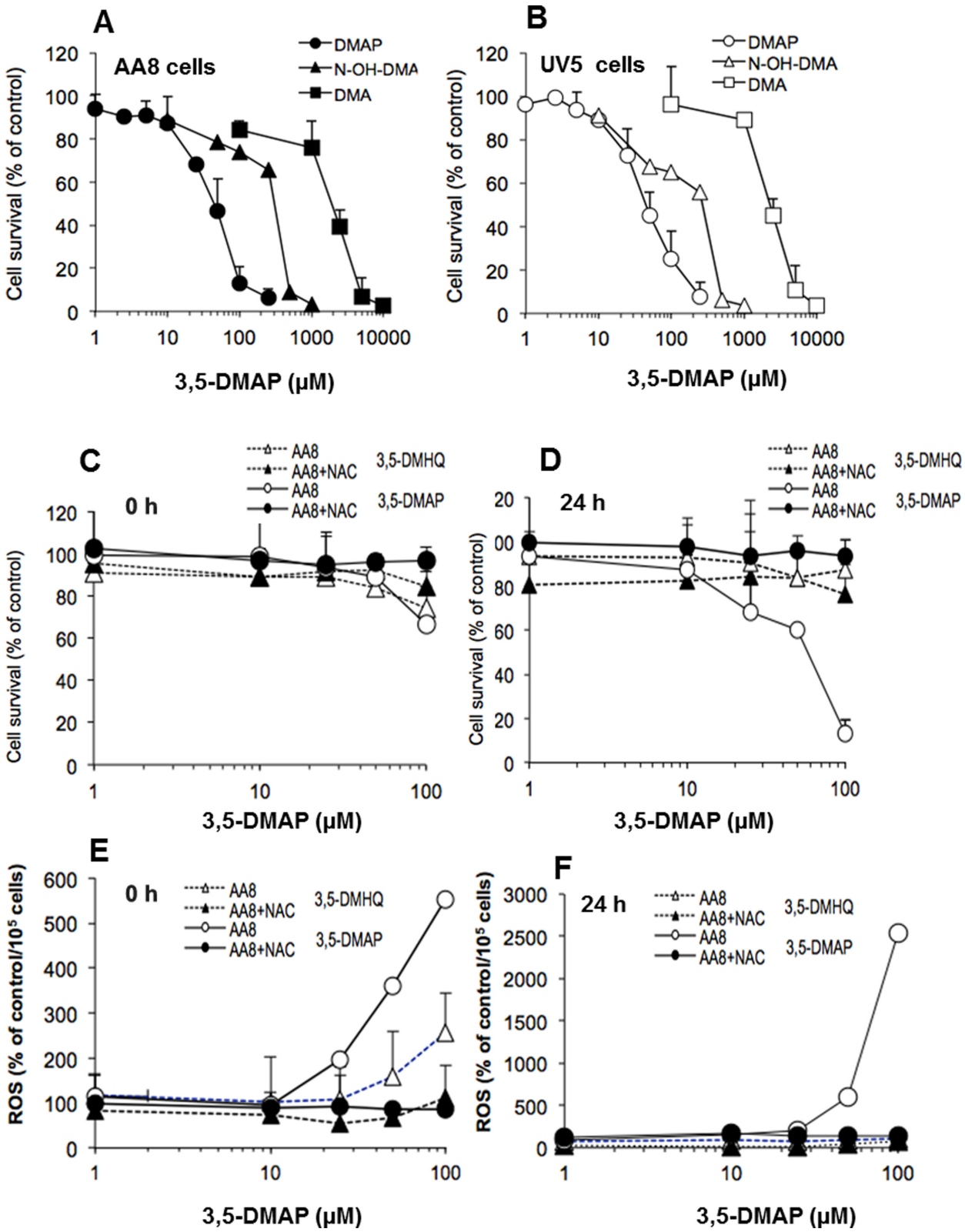

FIG. 2. Cytotoxicity of 3,5-DMA and its metabolites in AA8 and UV5 cells. (A) Cytotoxicity of 3,5-DMA and its metabolites NOH-3,5-DMA and 3,5-DMAP in AA8 cells. (B) Cytotoxicity of 3,5-DMA and its metabolites NOH-3,5-DMA and 3,5-DMAP in UV5 cells. (C) Cell survival of AA8 cells after treatment with 3-DMHQ plus NAC or 3,5-DMAP plus NAC at 0 h. (D) Cell survival of AA8 cells after treatment with 3-DMHQ plus NAC or 3,5-DMAP plus NAC after 24 h. (E) ROS production of AA8 cells after treatment with 3-DMHQ plus NAC or 3,5-DMAP plus NAC at 0 h. (F) ROS production of AA8 cells after treatment with 3-DMHQ plus NAC or 3,5-DMAP plus NAC after 24 h. The results are given as the mean of three independent experiments and triplicate measurements. ROS values correspond to fluorescence intensity relative to control values after normalizing to viable cell numbers. The data are normalized to the control and presented as percentage of control. Comparable data for UV5 cells are given in the Supplementary information.

only marginally toxic at concentrations up to 100 μM. As expected, 3,5-DMHQ gave evidence of ROS generation immediately after cells were dosed but ROS generation at 24 h was substantially less than immediately after dosing. As noted previously with 3,5-DMAP, the presence of 5 mM NAC afforded nearly complete protection against cell death and decreased ROS levels at all doses of DMHQ.

Cytotoxicity and persistence of ROS generation were further investigated for both 3,5-DMAP and DMHQ. Results are given in Figure 3. The cell viability of AA8 cells decreased gradually in 7 days after they were exposed to 50μM of 3,5-DMAP. Only 25% of the cells were viable versus control on day 3 and 10% of the cells were viable versus control on the seventh day (Fig. 3A). After 3,5-DMAP treatment, ROS production peaked at day 1 and remained above control levels for 7 days (600% of the control on day 1). ROS levels decreased gradually after the first day (Fig. 3B). In marked contrast, cell survival following treatment with the same concentration of 3,5-DMHQ remained 80% of the control (Fig. 3A). After the fifth day, cell viability showed significant increases, reaching control levels at day 7. After 3,5-DMHQ treatment, ROS production remained at control levels for 7 days (Fig. 3B). Figure 3C depicts image acquired at various times after exposing AA8 cells with 50-μM 3,5-DMAP for 1 h. Immediately after ($t = 0$), ROS and nuclear staining merge in some locations but ROS staining is not confined to areas where nuclear staining occurs. From 24 to 72 h, comparable with the data shown in Figure 3C, there is a high degree of overlap of nuclear and ROS staining. At 120 h, ROS staining is too weak to indicate with confidence whether it coincides with nuclear staining. The ROS staining disappears entirely at 168 h.

Intracellular Localization of ROS Produced by 3,5-DMAP

Intracellular localization of ROS was investigated first by imaging cells with epifluorescence microscopy at various times after exposure to 50 μM 3,5-DMAP in the absence and presence of NAC. Figure 4 shows data at 24 h after a 1-h exposure. Only 5% of control cells treated with DMSO showed evidence of ROS. After exposure to 50 μM 3,5-DMAP, 80% of cells were fluorescent (Fig. 4F). When cells were treated with 50-μM 3,5-DMAP plus 5 mM NAC or with 5 mM NAC alone, ROS production was undetectable. Responses were the same in AA8 and UV5 cells. A circumscribed image of cells treated with 3,5-DMAP alone was magnified and is shown in Figure 4D along with an image of cells treated with H_2O_2 (Fig. 4E). In both cases, it appears that ROS production occurs in both nucleus and cytoplasm.

The foregoing results did not reveal whether ROS were present within nuclei. To address this question, confocal microscopy was used to acquire images at 1.5-μm intervals of depth through selected AA8 cells that displayed overlapping nuclear and ROS staining (Supplementary fig. 2). From these series of images, we may interpret these results as evidence of 3,5-DMAP-induced-ROS production within the cell nucleus. This finding might account for its presumptive genotoxic and cytotoxic effects.

Effects of 3,5-DMAP on Glutathione Homeostasis

Table 1 summarizes total GSH, GSH, and GSSG levels with cellular redox ratios in both cytoplasmic and nuclear compartments of cells treated with 0–100-μM 3,5-DMAP for 1 h, then grown in the absence of the compound for 24 h. In the absence of NAC, both cytoplasmic and nuclear GSSG levels exhibited a dose-dependent increase with different 3,5-DMAP concentrations. Conversely, GSH concentrations declined with increasing doses of 3,5-DMAP. In the presence of NAC with 3,5-DMAP, however, GSH levels were significantly higher compared with the same dose of only 3,5-DMAP-applied group. Values of [GSH]/[GSSG] indicate a large shift in redox state for this couple as a result of 3,5-DMAP treatment that is similar in the absence or presence of NAC with respect to dose responsiveness. Activity of GR, a critical mediator of the intracellular [GSH]/[GSSG] ratio, was also determined. GR activity 24 h after exposure of cells to 5 and 10 μM showed no significant changes, whereas 25- and 50-μM doses caused decreases to 40% and 60% of control, respectively (Fig. 5A). When NAC was given along with 3,5-DMAP, GR activity was significantly higher when compared with only 3,5-DMAP-applied both AA8 and UV5 cells. 3,5-DMAP treatment of both AA8 and UV5 cells causes increases in SOD activity. The increase was more noticeable at doses >10 μM of 3,5-DMAP and reached as high as 30 μmol/mg at 50 μM (Fig. 5B). The increase in SOD activity caused by 3,5-DMAP was significantly decreased in the presence of NAC. These findings demonstrate that 3,5-DMAP induces ROS production and causes cellular toxicity in both AA8 and UV5 cells.

Product Markers of Intracellular ROS Generation

Products of the reaction of ROS with intracellular molecules other than GSH were also measured. The TBARS assay was used as an index of LP. In the present context, where there is independent evidence for extensive generation of ROS, increases in TBARS may reasonably be considered as reflective of LP products including Malondialdehyde Assay (MDA). Protein carbonyls were also assayed as an indicator of protein oxidation. Assays were conducted independently on cytoplasmic and nuclear fractions. Data from both assays are shown in Figures 5C–5F. Nuclear fractions generally gave lower values than cytoplasmic fractions but the overall pattern of responses to various treatments was similar. Exposure to 25-μM 3,5-DMAP increased TBARS about 4-fold in the cytoplasm and 9-fold in the nucleus, and protein carbonyls about 2-fold and 1.5-fold, respectively. All increases were statistically significant. Ascorbate alone neither reduced nor increased control values of TBARS or protein carbonyls significantly in both nuclear and cytoplasmic fractions. NAC only reduced nuclear protein carbonyl levels when applied alone. When 3,5-DMAP-treated cells were also given ascorbate plus 3,5-DMAP or NAC plus 3,5-DMAP, which are protective against 3,5-DMAP toxicity (Chao *et al.*, 2012), levels were reduced to control values except for nuclear TBARS, which were reduced but to a lesser extent.

Apoptotic Response to 3,5-DMAP

To characterize further mechanisms resulting in cell death caused by exposure to 3,5-DMAP, apoptotic cells were identified by flow cytometric analysis of cells after Annexin V-FITC and PI staining. The treatment protocol used was the same as that described above, involving exposure to 3,5-DMAP for 1 h, after which cells were collected, washed, and re-plated in fresh medium. After 24 h, treated AA8 cells (Fig. 6A) and UV5 cells (Supplementary fig. 3) showed a dose-dependent increase in apoptosis. When cells in early and late apoptosis are combined, doses of 50 and 100μM caused marked increases in apoptosis, reaching a maximum of nearly 100% in both cell types (Fig. 6B). Additional experiments were also performed and Western blot analyses showing the inverse dose-response relationship between 3,5-DMAP and pro-caspase 3, and between 3,5-DMAP and pro-PARP, as well as the protective effect of NAC is shown in Figure 7. Both AA8 and UV5 cells responded with about a 3-fold increase of caspase-3 activity 24 h after exposure to 3,5-DMAP doses from 10 to 50μM (Fig. 7A). This response was completely

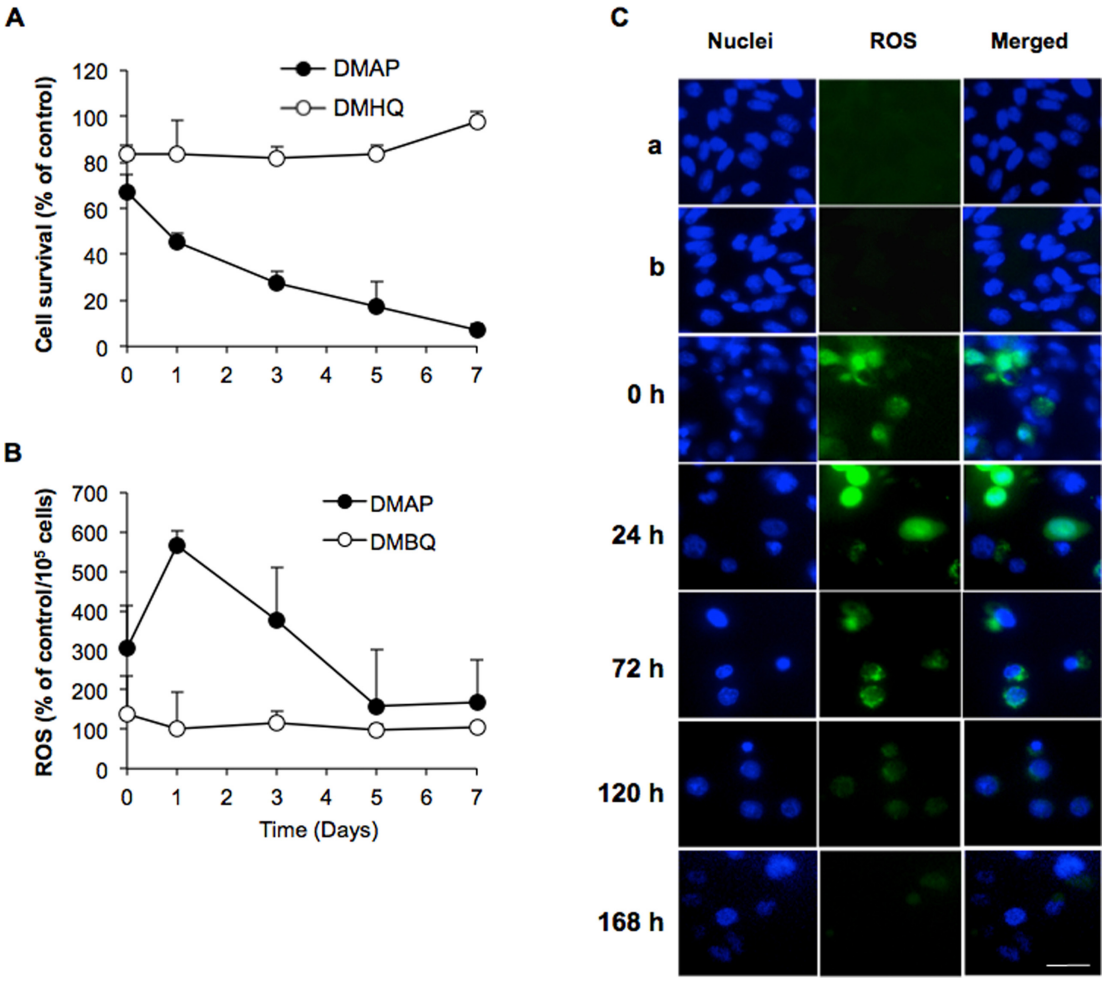

FIG. 3. Cytotoxicity and persistence of ROS generation were further investigated for both aminophenol and hydroquinone. (A) and (B) are long-term effects of 50-μM 3,5-DMAP and 3,5-DMHQ on ROS production and cell survival for AA8 cells. (C) Epifluorescence microscopy of AA8 cells at various times following treatment with 50-μM 3,5-DMAP. a: untreated cells; b: 50-μM 3,5-DMAP + 5 mM NAC: Immediately following treatment (0 h) ROS staining does not appear to co-localize with nuclear staining; however, by 24 h, there is a high degree of overlap, which remains apparent through 72 h. At 168 h, ROS staining is no longer apparent. Scale bar is 10 μm. Magnification is ×200.

TABLE 1. Cytopasmic and Nuclear Total, Oxidized, and Reduced Glutathione Levels in Study Groups

	Cytoplasmic				Nuclear			
3,5-DMAP (μM)	Total glutathione (nmol/mg protein)	GSSG (nmol/mg protein)	GSH (nmol/mg protein)	Redox ratio ([GSH]/[GSSG])	Total glutathione (nmol/mg protein)	GSSG (nmol/mg protein)	GSH (nmol/mg protein)	Redox ratio ([GSH]/[GSSG])
Control	15.8 ± 0.6	1.5 ± 0.1	12.8 ± 0.5	46.4 ± 3.6	5.4 ± 0.4	0.3 ± 0.1	4.8 ± 0.	16.0 ± 1.0
NAC	20.9 ± 0.2*	1.2 ± 0.2*	18.4 ± 0.2*	77.0 ± 8.5*,#	7.4 ± 0.2*	0.3 ± 0.1*	6.9 ± 0.2*	27.3 ± 1.5*
10	16.2 ± 0.7	1.6 ± 0.1	12.9 ± 0.6	42.2 ± 1.7	6.3 ± 0.1*	0.4 ± 0.1	5.5 ± 0.1*	16.4 ± 0.2
10+NAC	23.1 ± 0.6*,#	1.6 ± 0.4	19.9 ± 1.0*,#	77.0 ± 5.8*,#	8.5 ± 0.3*,#	0.3 ± 0.0#	7.9 ± 0.3*,#	28.4 ± 2.3*,#
25	16.7 ± 0.8	2.1 ± 0.4*	12.5 ± 1.0	28.6 ± 0.5*	6.5 ± 0.1*	0.6 ± 0.1*	5.4 ± 0.4	11.2 ± 0.3*
25+NAC	21.1 ± 1.6*,#	1.6 ± 0.1*,#	17.8 ± 1.7*,#	53.1 ± 4.5	8.2 ± 0.2*,#	0.4 ± 0.0*,#	7.4 ± 0.2*,#	20.4 ± 0.8*,#
50	19.3 ± 1.4*	6.5 ± 0.1*	6.3 ± 1.5*	10.5 ± 0.4*	7.7 ± 0.4*	1.8 ± 0.0*	4.1 ± 0.4*	4.2 ± 0.2*
50+NAC	21.8 ± 1.1*,#	5.1 ± 0.3*,#	11.6 ± 1.6*,#	20.5 ± 0.6*,#	8.9 ± 0.3*,#	1.1 ± 0.0*,#	6.7 ± 0.3*,#	8.3 ± 0.7*,#
100	20.3 ± 0.5*	8.0 ± 0.2*	4.3 ± 0.7*	7.4 ± 0.6*	8.5 ± 0.7*	2.7 ± 0.0*	3.0 ± 0.7*	3.1 ± 0.2*
100+NAC	20.1 ± 0.7*	6.8 ± 0.3*,#	6.6 ± 1.3*,#	10.2 ± 0.2*	9.4 ± 0.3*,#	2.0 ± 0.1*,#	5.5 ± 0.2*,#	4.8 ± 0.3*,#

GSH, reduced glutathione; GSSG, oxidized glutathione. Redox ratio ([GSH]/[GSSG]) is calculated by dividing GSH levels into GSSG levels. The results are presented as means ± SD of three independent experiments and duplicate measurements.

*$p < 0.05$ indicates that the mean is significantly different from control group.

#$p < 0.05$ indicates that the mean of the NAC plus 3,5-DMAP-applied group is significantly different from the same dose of the 3,5-DMAP-applied group.

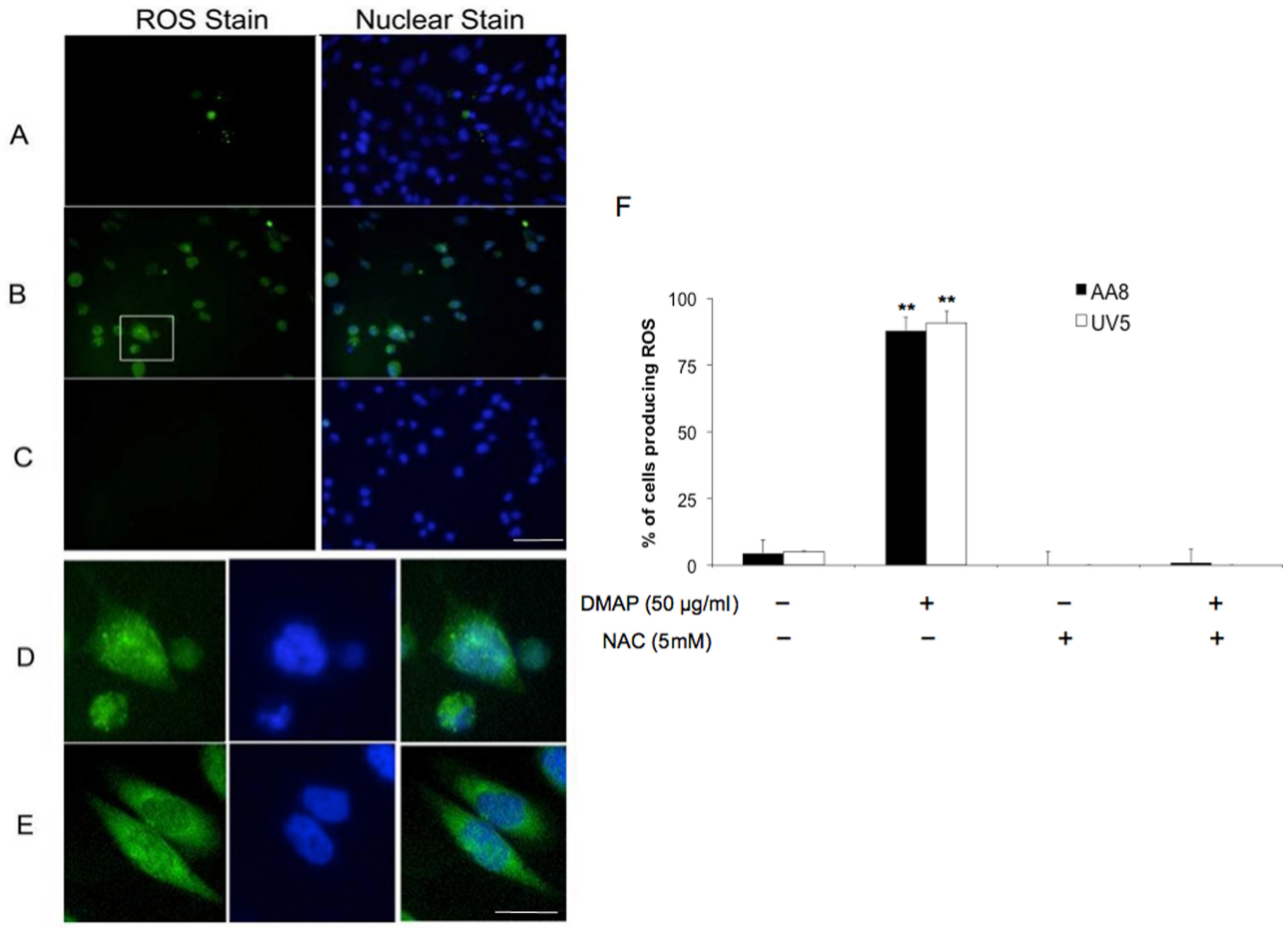

FIG. 4. Epifluorescence microscopy of AA8 cells treated with 3,5-DMAP. Comparable data for UV5 cells are given in the Supplementary information. (A) untreated AA8 cells, (B) AA8 cells treated with 50 μM 3,5-DMAP, and (C) AA8 cells treated with 50 μM 3,5-DMAP + 5 mM NAC. At this level of magnification, ROS and nuclear staining are almost completely coincident. Scale bar is 30 μm. (D) The highlighted area is shown at higher magnification in (B). (E) A comparison with results from the 10 mM H_2O_2 treatment, and both treatments appear to generate ROS throughout the cell. Cells treated with 5 mM NAC in the absence of 3,5-DMAP exhibited negligible ROS staining. Scale bar is 5 μm. (F) Quantitation of ROS detection after 3,5-DMAP exposure. Values were divided by the amount of nuclei stain in the assessed region to attain the number of ROS per 100 cells. The values are normalized to the control and showed as the percentage change relative to control. The results are presented as means ± SD of three independent experiments and duplicate measurements. Significant differences from control values are indicated with $^{**}p < 0.01$.

blocked by simultaneous exposure to 5-mM NAC. Caspase-3 activity increased steadily over a 24-h period following treatment with 50-μM 3,5-DMAP (Fig. 7B). Caspase-3 activation was entirely blocked in the cells co-treated with 5-mM NAC. These findings are confirmed and extended by Western blot analyses showing an inverse dose-response relationship between 3,5-DMAP and pro-caspase 3, and between 3,5-DMAP and pro-PARP, the protein target of caspase 3 (Fig. 7C). In the presence of 5-mM NAC both pro-caspase 3 and pro-PARP levels remained unchanged after exposure to 3,5-DMAP.

Mitigation of 3,5-DMAP Cytotoxicity by ROS Scavengers

To explore the relationship between ROS generation by 3,5-DMAP and cytotoxicity, viable cell numbers were enumerated 24 h after a 1-h exposure to 50-μM 3,5-DMAP in the presence or absence of the ROS scavengers NAC, ascorbate, SOD, CAT, SOD/CAT, uric acid, and Tiron. Table 2 summarizes the results.

NER is a highly versatile and sophisticated DNA damage removal pathway that counteracts the deleterious effects of a wide variety of DNA lesions, including UV-induced cyclobutane pyrimidine dimers and photoproducts and numerous bulky chemical adducts (de Laat *et al.*, 1999). Responses of the two cell types to each treatment were essentially identical, indicating that NER DNA repair status had negligible influence on processes leading to cell death. Exposure to 50 μM 3,5-DMAP alone caused about 60% lethality in both cell types. As observed previously (Chao *et al.*, 2012), co-treatment with 5 mM NAC completely abrogated the cytotoxic effects of 3,5-DMAP ($p < 0.05$, compared with control cells). Ascorbate was moderately protective ($p < 0.05$ vs. control cells) at 50 mg/ml, which is a concentration relevant to physiological levels. 3,5-DMAP in combination with SOD (50–1000 U) caused nearly 60% of both cell types to die. There is no significant difference between a low dose of CAT (50 U) alone and co-treatment with CAT (50 U) + SOD (50 U) in 3,5-DMAP-induced AA8 and UV5 cells. There was merely about a 40% survival rate. Although the cells treated with 500 and 1000 U of CAT or 1000 U of both SOD + CAT survival rates increased to 50% and 65%, respectively ($p < 0.05$ vs. control cells). Uric acid at 0.5mM and 5mM reduced lethality to 10% and 30% ($p < 0.05$ vs. control cells), respectively, but a higher concentration proved ineffective, perhaps by contributing for an additional toxic effect. The $O_2^{\cdot -}$ scavenger Tiron (0.5–50mM) provided a minor degree of protection, increasing survival by about 10% at the highest dose ($p > 0.05$, compared with control cells).

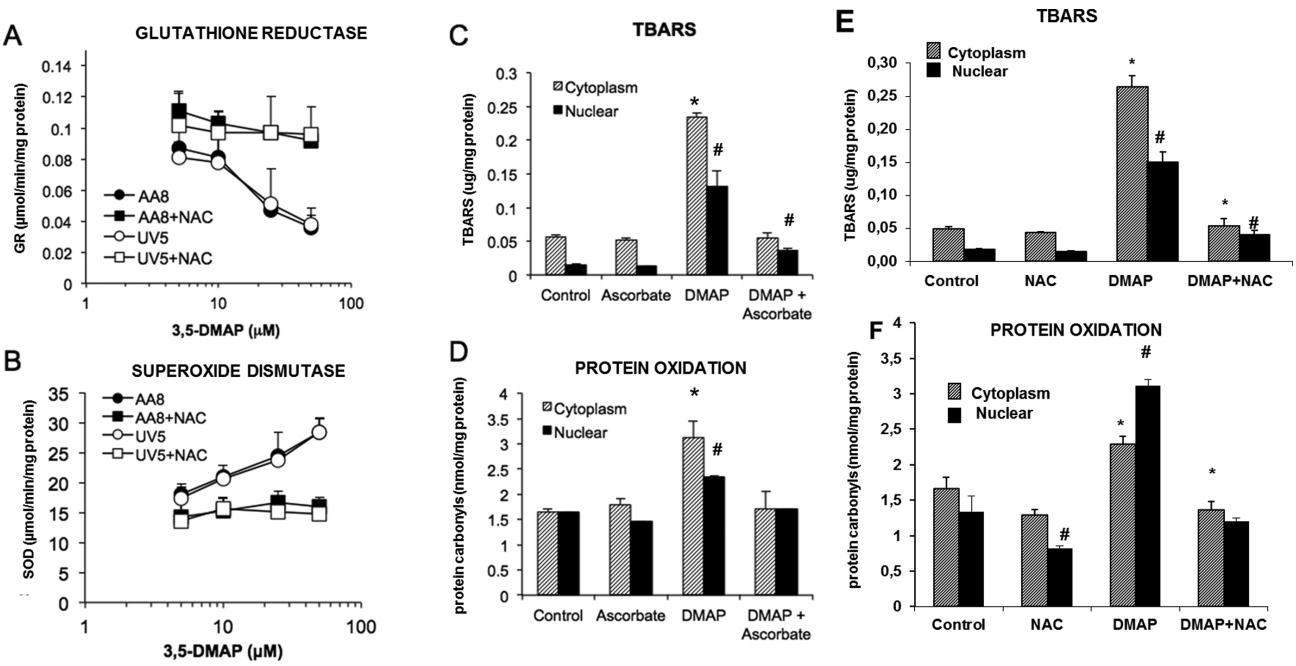

FIG. 5. Response of intracellular GR and SOD activity and ROS product markers following exposure to 3,5-DMAP. (A) GR: glutathione reductase in AA8 and UV5 cells with 3,5-DMAP (25 μM) ± NAC (5mM). (B) SOD: superoxide dismutase in AA8 and UV5 cells with 3,5-DMAP (25μM) ± NAC (5 mM). (C) lipid peroxidation (LP as TBARS) after exposure to 3,5-DMAP (25 μM) ± ascorbate (50 μg/ml). (D) protein oxidation (protein carbonyls) after exposure to 3,5-DMAP (25 μM) ± ascorbate (50 μg/ml). (E) lipid peroxidation (LP as TBARS) after exposure to 3,5-DMAP (25 μM) ± NAC. (F) protein oxidation (protein carbonyls) after exposure to 3,5-DMAP (25 μM) ± NAC. TBARS: thiobarbituric acid reactive substance. The results are presented as means ± SD of three independent experiments and duplicate measurements. *Cytoplasmic LP or protein oxidation levels are significantly higher compared with control ($p < 0.05$). #Nuclear LP or protein oxidation levels are significantly higher compared with control ($p < 0.05$).

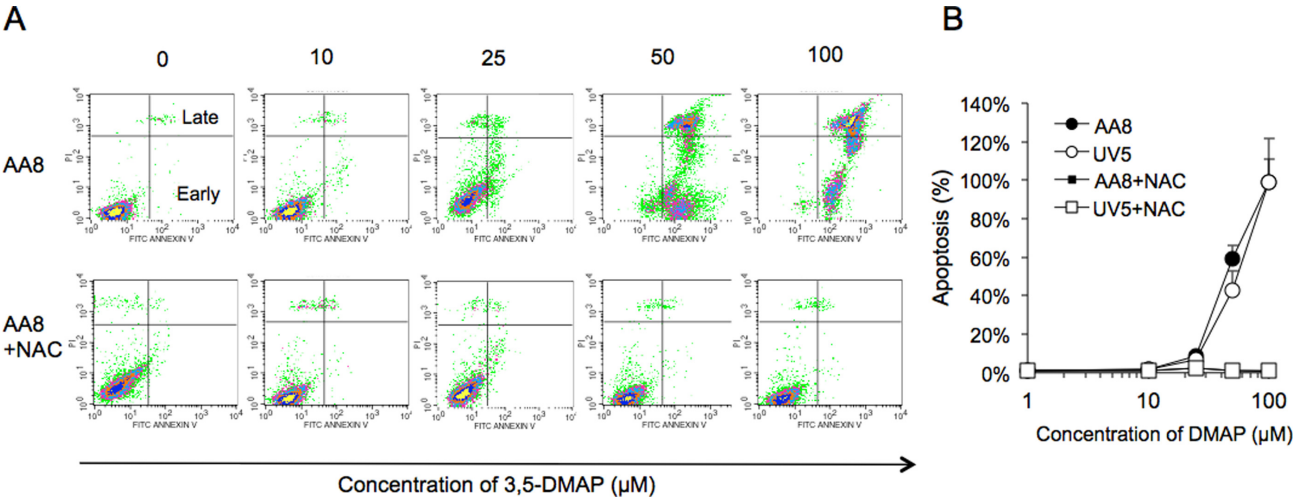

FIG. 6. Apoptotic cells were identified by flow cytometric analysis of cells after Annexin V-FITC and PI staining (A). The analysis of AA8 cells treated with 3,5-DMAP (0, 10, 25, 50, and 100μM) ± NAC (5mM) for 24 h (A). (B) Dose responses based on all data are plotted. Top and right of the graphs on panel (A) indicate late apoptosis and below of right part indicates early apoptosis as also shown. Panel (A) shows the data including normal cells, necrotic cells, early apoptotic, and late apoptotic cells with histogram plotting. Panel (B) shows a quantitation of the total apoptosis results (early + late) generated from panel (A) and suggests that the changes in apoptosis is dose related in both AA8 and UV5 cells. When the concentration of 3,5-DMAP is increased, cells are more late apoptotic. NAC seems to be protective for both of the cell types and protects the viability of the cells.

3,5-DMAP Induces H_2O_2 and ·OH Production and Upregulates Caspase 3 in AA8 and UV5 Cells

To sequentially evaluate which free radical plays a key role to cause 3,5-DMAP toxicity, assays were repeated with the addition to medium of NAC (5 mM), SOD (1000 U), CAT (1000 U), SOD + CAT (both in 1000 U), Tiron (0.5 mM), and uric acid (5 mM) along with the 50 μM 3,5-DMAP employed. As shown in Figure 8A, H_2O_2 was detected with "Fluoro H_2O_2 Hydrogen Peroxide Assay kit" under 3,5-DMAP and ROS scavengers exposure. H_2O_2 was increased to 10-fold of control at both 3,5-DMAP alone and 3,5-DMAP plus SOD in AA8 cells (black bars, $p < 0.05$ vs. control, both). Although the production was blocked by co-treating with NAC ($p > 0.05$ vs. control), CAT, and SOD/CAT, however, scavenging $O_2\cdot^-$ with Tiron showed no decrease of H_2O_2 production. CAT reduced sig-

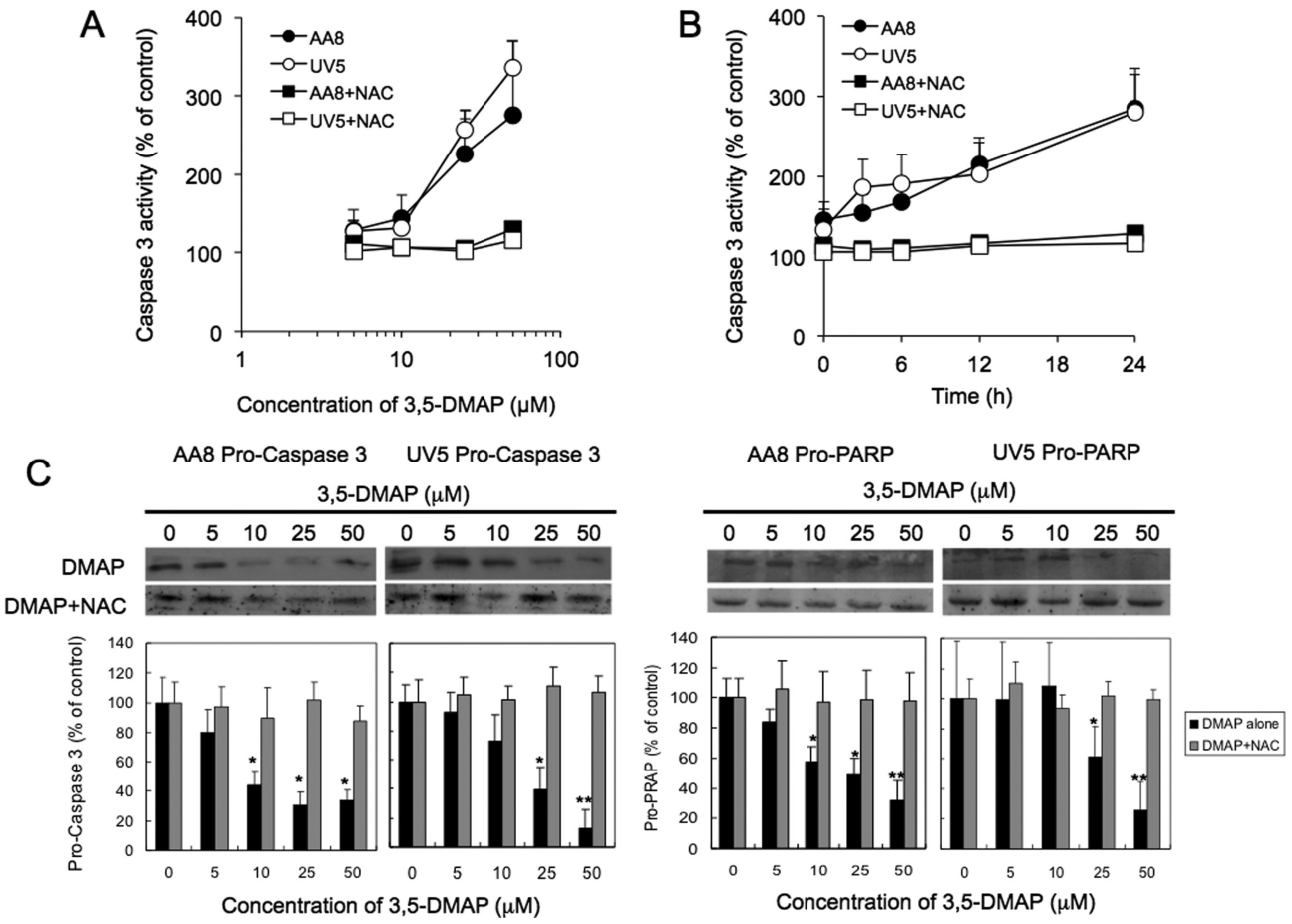

FIG. 7. Apoptotic marker caspase-3 assay shows the inverse dose- (A) and time-response (B) relationship between 3,5-DMAP and caspase-3 activity. (C) Western blot suggests that ROS induced by 3,5-DMAP exposure induces pro-caspase-3 and pro-PARP expression in AA8 and UV5 cells. NAC diminished these responses. Significant differences from control values are indicated with $^{*}p < 0.05$ and $^{**}p < 0.01$.

TABLE 2. Survival of AA8 and UV5 Cells Treated with 50μM of 3,5-DMAP Plus ROS Scavengers at the Density of 1×10^6 Cells

	AA8		UV5	
Chemicals	Concentration	Survival (%)	Concentration	Survival (%)
Control		100 ± 1.7		100 ± 6.1
DMAP only	50 uM	40 ± 6.2	50 uM	36 ± 2.6
NAC	5 mM	100 ± 11.3*	5 mM	99 ± 9.4*
Ascorbate	50 ug/ml	59 ± 12*	50 ug/ml	57 ± 5.9*
SOD	50 U	33 ± 0.4	50 U	35 ± 4.1
	500 U	36 ± 3.8	500 U	35 ± 0.8
	1000 U	39 ± 4.5	1000 U	36 ± 2.3
CAT	50 U	39 ± 3.9	50 U	43 ± 2.4
	500 U	47 ± 0.7	500 U	59 ± 7.5
	1000 U	63 ± 3.9*	1000 U	70 ± 3.2*
SOD + CAT	50 U	38 ± 0.2	50 U	39 ± 3.6
	500 U	47 ± 1.4	500 U	50 ± 4.2
	1000 U	62 ± 5.6*	1000 U	67 ± 1.7*
Uric acid	0.5 mM	72 ± 4.8*	0.5 mM	76 ± 4.4*
	5 mM	88 ± 15.4*	5 mM	93 ± 18.3*
	50 mM	43 ± 6.9	50 mM	45 ± 16.1
Tiron	0.5 mM	45 ± 0.7	0.5 mM	40 ± 2.1
	5 mM	50 ± 2.9	5 mM	34 ± 5.4
	50 mM	52 ± 3.2	50 mM	50 ± 8.2*

The results are presented as means ± SD of three independent experiments and triplicate measurements. The survival rate in each assay was calculated and normalized to untreated control. U of SOD and CAT means units/ml. Significant differences between samples and 3,5-DMAP-treated sample values are indicated with $^{*}p < 0.05$.

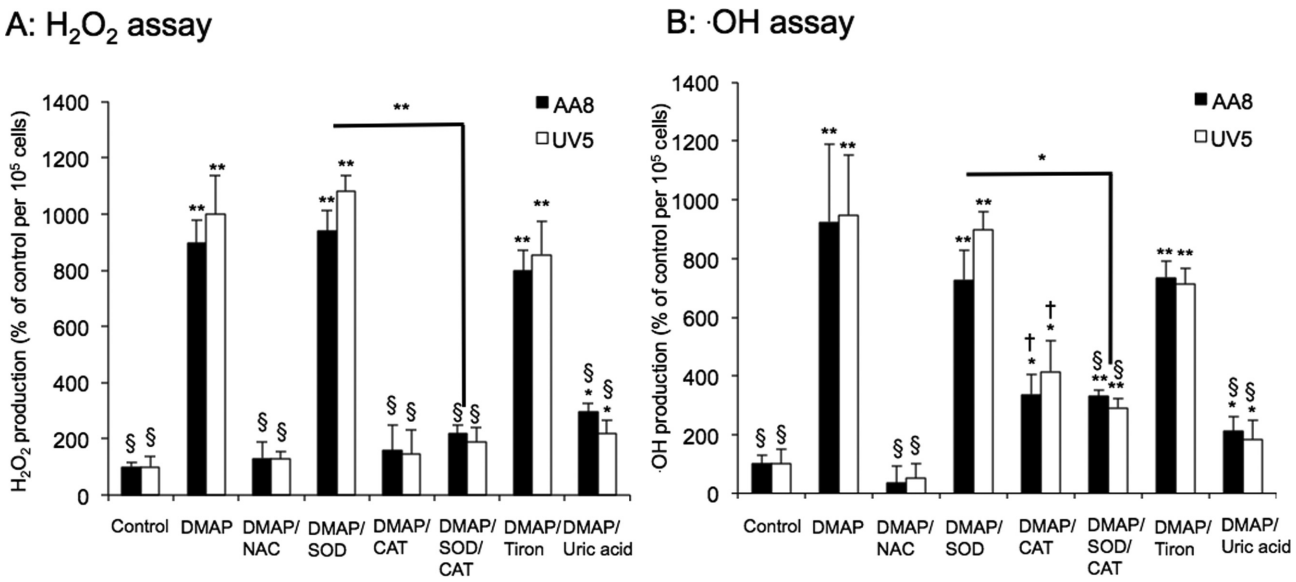

FIG. 8. 3,5-DMAP generates H_2O_2 and ·OH production in AA8 and UV5 cells. (A) Measurement of H_2O_2 and (B) ·OH production in the AA8 and UV5 cells treated with 3,5-DMAP (50 μM) with or without ROS scavengers [NAC (5 mM), SOD (1000 U), CAT (1000 U), SOD/CAT (both in 1000 U), Tiron (0.5 mM), and uric acid (5 mM)] using the DAF-DA method and the HPF method, respectively. The cell treated with DMSO is defined as the negative control. The results are presented as means ± SD of three independent experiments and duplicate measurements. The results are normalized to the control. Significant differences from control values are indicated with $^*p < 0.05$ and $^{**}p < 0.01$, and from 3,5-DMAP samples † is $p < 0.01$ and § is $p < 0.001$.

nificant H_2O_2 levels produced from 3,5-DMAP plus SOD ($p < 0.01$ vs. control). Furthermore, addition of uric acid reduced the H_2O_2 level from 900% to 200%, however, it cannot diminish entirely H_2O_2 produced from 3,5-DMAP in both cells ($p = 0.02$ at AA8, $p = 0.02$ at UV5 cells vs. controls). Figure 8B shows that 3,5-DMAP alone and 3,5-DMAP plus SOD cause about 9-fold and 8-fold ·OH production increase of control in both AA8 and UV5 cells, respectively, determined using with HPF assay kit. In combination with other free radical scavengers, NAC entirely inhibits ·OH generation ($p < 0.05$ vs. 3,5-DMAP-applied cells), whereas CAT exerted suppression of ·OH generation but remained about 4-fold increase (2.5-fold decrease from 3,5-DMAP alone), and no significant difference was observed under the co-treatment with SOD/CAT and Tiron. By comparing 3,5-DMAP+SOD and 3,5-DMAP+SOD/CAT, we found CAT reduced significant ·OH amount produced from 3,5-DMAP plus SOD ($p < 0.05$). Uric acid functioned to eliminate the ·OH level from 9- to 2-fold of control, but there remained a significant elevation in the ·OH production compared with the control ($p = 0.0459$ at AA8 cells and $p = 0.0437$ at UV5 cells).

The data in Figure 7 demonstrated that 3,5-DMAP activates caspase-3 activity which may eventually lead to apoptosis. We further investigated whether the H_2O_2 and ·OH generated from 3,5-DMAP induce caspase-3 activation. As shown in Figure 9, the cells treated with 50 μM 3,5-DMAP showed 280% increase of control caspase-3 activity ($p < 0.05$). 3,5-DMAP plus NAC significant suppressed caspase-3 activity. At the treatment with SOD, CAT, SOD/CAT, and Tiron, the caspase activity increased almost 300%, 220%, 250%, and 260% increase of control, respectively ($p < 0.05$ vs. control, all). Addition of uric acid significantly decreased 3,5-DMAP increased caspase-3 activity in both AA8 and UV5 cells. Although the caspase-3 activity for both AA8 and UV5 cells showed no difference compared with the control ($p = 0.12$ for AA8 cells and $p = 0.05$ at UV5 cells), they were significantly lower compared with 3,5-DMAP-treated cells ($p < 0.05$). These findings suggested that 3,5-DMAP was able to produce high levels of H_2O_2 and ·OH in AA8 and UV5 cells and caused apoptosis by activating caspase-3 pathway.

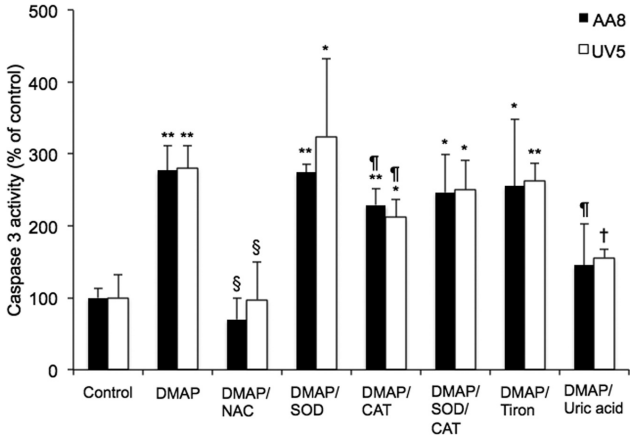

FIG. 9. The 3,5-DMAP-generated H_2O_2 and ·OH cause apoptosis by activating caspase 3. The results are presented as mean ± SD of three independent experiments and duplicate measurements. Significant differences from negative control values are indicated with $^*p < 0.05$ and $^{**}p < 0.01$. Significant differences relative to 3,5-DMAP sample: ¶ is $p < 0.05$, † is $p < 0.01$, and § is $p < 0.001$.

DISCUSSION

Previously, we have put forth and supported the hypothesis that certain alkylanilines exert genotoxic effects through ROS production by aminophenol metabolites and 3,5-DMAP became histone bound as N^{ϵ}-(4-hydroxy-3,5-dimethylphenyl)lysine when given to cells cultures (Chao *et al.*, 2012; Ye *et al.*, 2012). Here, we continue the experiments concerning cell viability after treatment of 3,5-DMA and its metabolites. This work suggests a diverse profile of cytotoxic potencies in both AA8 and UV5 cells: 3,5-DMAP has the highest potency and N-OH-DMA intermedi-

ate and 3,5-DMA the lowest. Our results show that aminophenols are mechanistically unique as redox-active compounds and ROS production can be mentioned among the underlying factors of the cytotoxicity of 3,5-DMAP. These findings prompted the more extensive characterization of intracellular ROS production by 3,5-DMAP, with the goals of characterizing the persistence of ROS production through cell growth and replication.

The previous study was limited to the 24-h period following withdrawal of 3,5-DMAP; focused on damage to DNA and ROS production was investigated within 24 h (Chao *et al.*, 2012). The present results show that the persistent, indeed, increased the production of ROS at this time relative to the period immediately after dosing (Fig. 2), indicating that 3,5-DMAP was binding to the intracellular matrix in a form capable of continued redox cycling. In addition, this study extended the investigated time period to 7 days. ROS production continued for at least the first five days at which point cell survival became too low for meaningful data analysis. These findings strongly indicate that intracellular ROS formation is an important, if not principal, mechanism by which aminophenols cause damage to DNA and to other cellular targets. Our results showed the ongoing toxicity of 3,5-DMAP over 7 days, whereas cell survival following treatment with 3,5-DMHQ remains unchanged over the same period (Fig. 3). Moreover, ROS production after 3,5-DMHQ treatment declines to control levels within 24 h, but remains elevated for several days following 3,5-DMAP treatment.

To our knowledge, this is the first study showing that antioxidants are capable of reducing the oxidative damage exerted by alkylanilines. There was a common relationship between the effects of 3,5-DMAP on GR and on GSH homeostasis in that both were negatively affected. Why GR was inhibited rather than induced by 3,5-DMAP treatment is not clear but preliminary experiments using mass spectrometry suggest that covalent binding of the aminophenol to the enzyme may play a role (Chao *et al.*, unpublished data). NAC both mitigated inhibition of GR activity by 3,5-DMAP and raised GSH/GSSG redox ratio at a given dose of 3,5-DMAP, as expected, if GR activity was a major determinant of GSSG levels (Table 1 and Fig. 5A). The effects of NAC on these two outcomes were dissimilar, however. GR activity was completely protected by NAC up to at least 50μM, whereas GSSG increased dramatically at this dose level. Apoptosis, cell survival, and mutagenicity were like GR activity, virtually identical to control values at all doses of 3,5-DMAP in the presence of NAC (Chao *et al.*, 2012). Therefore, NAC may act partly as a nucleophilic scavenger, reacting with the quinone imine form of 3,5-DMAP through Michael addition to inactivate it with respect to transimination. Additionally, NAC might serve the same function as GSH in maintaining the intracellular redox environment—it possesses the same redox couple—without the need for a reductase because NAC in the growth medium serves as a reservoir of free thiol that is very large relative to the intracellular pool. The limited protection of GSH by NAC with high doses of 3,5-DMAP can be interpreted as the result of GR inactivation, which, if it occurs by electrophilic attack on the enzyme, is unlikely to be significantly mitigated by NAC because small molecules are generally poor competitors compared with proteins (Skipper, 1996). SOD activity increased after 3,5-DMAP exposure (Fig. 5B). SOD activity elevation after 3,5-DMAP treatments was more noticeable at doses <10μM, whereas the activity of this particular enzyme was significantly reduced by NAC. Several ROS scavengers were also administered against the toxicity of 3,5-DMAP (Table 2). Uric acid was highly effective at 5mM, but toxic at the highest dose tested. Although the antioxidant potential of uric acid was reported that high dose uric acid might act as a pro-oxidant (Proctor, 2008). This phenomenon might explain the observation that high-dose uric acid caused cytotoxicity. Ascorbate, CAT, and SOD/CAT were moderately effective and Tiron exhibited only borderline protection. However, there is no difference between 3,5-DMAP alone and 3,5-DMAP plus SOD as well. These results suggest three possibilities: First, 3,5-DMAP might remain to induce amount of $O_2\cdot^-$ production, however, $O_2\cdot^-$ was dismutated and generated H_2O_2 when SOD was used (Li *et al.*, 1996). Second, mitochondria might release some $O_2\cdot$, which was scavenged by SOD to generate more H_2O_2 as well. Third, ·OH might be a third free radical produced in this system.

The increased intracellular level of LP is a good indicator of intracellular oxidation (Mateos and Bravo, 2007). LP by-products can attack several cellular targets, like proteins (Emerit *et al.*, 1991). Concerning our findings, we can postulate that protein oxidation elevation by DMAP might be a secondary effect of LP. Because quinones are also capable of binding to proteins (through Michael addition of cysteine sulfhydryls), it was of interest to compare the structurally analogous 3,5-DMHQ with 3,5-DMAP (which is capable of both transimination and Michael addition). Our results suggest that there are fewer cellular targets for 3,5-DMHQ and/or that it is less efficient at producing ROS (Fig. 2) because:

- ROS production is less than with 3,5-DMAP at 0 and 24 h;
- ROS production is lower rather than higher at 24 h as compared with 0 h;
- It is less toxic.

We suggest that 3,5-DMAP produces both H_2O_2 and ·OH in the cells (Fig. 8). By combining the data with Table 2, we found that 3,5-DMAP at 50-μM 60% cell death seems to be accomplished by 40% from ·OH and 20% from H_2O_2. Figure 9 shows a similar demonstration as well that CAT is able to reduce caspase-3 activation from 277% to 229% (AA8, $p = 0.0161$) and 280% to 211% (UV5, $p = 0.0145$) of control. But the ·OH upregulates pro-caspase-3 expression and apoptotic cell death is possibly induced by the activation of the zymogen pro-caspase 3 to caspase 3. SOD and CAT were not effective in reducing oxidation by 3,5-DMAP and H_2O_2 was produced as high as 3,5-DMAP treatment alone. After CAT joined to the system (3,5-DMAP plus SOD/CAT), CAT blocks H_2O_2 production, but caspase-3 activity did not decrease. Addition of NAC provided a 100% inhibition of both ROS production and cytotoxicity, whereas uric acid did not. After uric acid co-treatment, H_2O_2 and ·OH were produced to a lesser extent and this compound slightly induced caspase-3 activity which resulted in 88% ± 15.4% and 93% ± 18.3% cell survival in AA8 and UV5 cells, respectively. The reason might be that NAC is a stronger electron donor and it provides higher protection potential than uric acid (Krasowska and Konat, 2004). The prolonged intracellular ROS production and concomitant cytotoxicity are a signal property of 3,5-DMAP and by extension, perhaps, other aminophenols. These compounds are cytotoxic and have been shown to produce DNA damage in the form of strand breaks.

The concerted action of caspases is responsible for apoptosis (Dang, 2012). When activated, the extrinsic pathway, which includes the action of initiator caspases 8 and 10, cleaves and activates the executioner caspases 3 and 7. It was demonstrated that oxidative stress could activate caspase 8 (Boatright and Salvesen, 2003). After 3,5-DMAP exposure, apoptosis was virtually the sole mechanism responsible for loss of viability, and the common response of the two cell lines with respect to apoptosis, DNA strand breakage, and protection by ROS scavengers is not protective, but rather favors oxidative DNA damage as one of the

principal toxicity mechanisms. Though it is not feasible to draw clear conclusions from the presented data, the results evoke oxidative damage as an important, if not predominant, mechanism underlying the apoptotic effect of 3,5-DMAP. Additionally, this mechanism is further supported by the results showing the effect of NAC in maintaining expression of pro-caspase 3 and pro-PARP and in inhibiting caspase-3 activity (Fig. 7). Although it remains to be determined whether ROS produced by embedded aminophenol structures are actual toxicants, the apoptotic response reported herein is a further indicator of DNA damage.

In conclusion, this is the first study showing that antioxidants, particularly NAC, are protective against oxidative potential of 3,5-DMAP. This study also provides a more mechanistical approach for the cytotoxic potential of 2,6-DMA and its metabolites. 3,5-DMAP seems to affect the GSH pathway, increase SOD activity, and induce caspase-3 activity. Apoptosis seems to be the major form of cell death caused by 3,5-DMAP and NAC was found to be protective against its toxic potential. The results presented herein emphasize the importance of antioxidants, with respect to the high probability of alkylaniline exposures and their toxic effects.

SUPPLEMENTARY DATA

Supplementary data are available online at http://toxsci.oxfordjournals.org/.

FUNDING

National Institute of Environmental Health Science (P01-ES006052 and ES02109).

REFERENCES

Akerboom, T. P. and Sies, H. (1981). Assay of glutathione, glutathione disulfide, and glutathione mixed disulfides in biological samples. *Methods Enzymol.* **77**, 373–382.

Barreto, G., Madureira, D., Capani, F., Aon-Bertolino, L., Saraceno, E. and Alvarez-Giraldez, L. D. (2009). The role of catechols and free radicals in benzene toxicity: an oxidative DNA damage pathway. *Environ. Mol. Mutagen.* **50**, 771–780.

Boatright, K. M. and Salvesen, G. S. (2003). Mechanisms of caspase activation. *Curr. Opin. Cell Biol.* **15**, 725–731.

Bolton, J. L., Trush, M. A., Penning, T. M., Dryhurst, G. and Monks, T. J. (2000). Role of quinones in toxicology. *Chem. Res. Toxicol.* **13**, 135–160.

Bomhard, E. M. and Herbold, B. A. (2005). Genotoxic activities of aniline and its metabolites and their relationship to the carcinogenicity of aniline in the spleen of rats. *Crit. Rev. Toxicol.* **35**, 783–835.

Breimer, L. H. (1990). Molecular mechanisms of oxygen radical carcinogenesis and mutagenesis: The role of DNA base damage. *Mol. Carcinog.* **3**, 188–197.

Chao, M. W., Kim, M. Y., Ye, W., Ge, J., Trudel, L. J., Belanger, C. L., Skipper, P. L., Engelward, B. P., Tannenbaum, S. R. and Wogan, G. N. (2012). Genotoxicity of 2,6- and 3,5-dimethylaniline in cultured mammalian cells: The role of reactive oxygen species. *Toxicol. Sci.* **130**, 48–59.

Cui, L., Sun, H. L., Wishnok, J. S., Tannenbaum, S. R. and Skipper, P. L. (2007). Identification of adducts formed by reaction of N-acetoxy-3,5-dimethylaniline with DNA. *Chem. Res. Toxicol.* **20**, 1730–1736.

Dang, T. P. (2012). Notch, apoptosis and cancer. *Adv. Exp. Med. Biol.* **727**, 199–209.

Emerit, I., Khan, S. H. and Esterbauer, H. (1991). Hydroxynonenal, a component of clastogenic factors? *Free Radic. Biol. Med.* **10**, 371–377.

Gan, J., Skipper, P. L., Gago-Dominguez, M., Arakawa, K., Ross, R. K., Yu, M. C. and Tannenbaum, S. R. (2004). Alkylaniline-hemoglobin adducts and risk of non-smoking-related bladder cancer. *J. Natl. Cancer Inst.* **96**, 1425–1431.

Gan, J., Skipper, P. L. and Tannenbaum, S. R. (2001). Oxidation of 2,6-dimethylaniline by recombinant human cytochrome P450s and human liver microsomes. *Chem. Res. Toxicol.* **14**, 672–677.

Van Hemelrijck, M. J., Michaud, D. S., Connolly, G. N. and Kabir, Z. (2009). Secondhand smoking, 4-aminobiphenyl, and bladder cancer: Two meta-analyses. *Cancer Epidemiol. Biomarkers Prev.* **18**, 1312–1320.

Hengstler, J. G. and Bolt, H. M. (2008). Oxidative stress: from modification of cell-cycle related events, secondary messenger function, dysregulation of small GTPases, protein kinases and phosphatases to redox-sensitive cancer models. *Arch.Toxicol.* **82**, 271–272.

Hill, B. A., Davison, K. L., Dulik, D. M., Monks, T. J. and Lau, S. S. (1994). Metabolism of 2-(glutathion-S-yl)hydroquinone and 2,3,5- (triglutathion-S-yl)hydroquinone in the in situ perfused rat kidney: Relationship to nephrotoxicity. *Toxicol. Appl. Pharmacol.* **129**, 121–132.

Hiraku, Y. and Kawanishi, S. (1996). Oxidative DNA damage and apoptosis induced by benzene metabolites. *Cancer Res.* **56**, 5172–5178.

Kim, D. and Guengerich, F. P. (2005). Cytochrome P450 activation of arylamines and heterocyclic amines. *Annu. Rev. Pharmacol. Toxicol.* **45**, 27–49.

Krasowska, A. and Konat, G. W. (2004). Vulnerability of brain tissue to inflammatory oxidant, hypochlorous acid. *Brain Res.* **997**, 176–184.

Kugler-Steigmeier, M. E., Friederich, U., Graf, U., Lutz, W. K., Maier, P. and Schlatter, C. (1989). Genotoxicity of aniline derivatives in various short-term tests. *Mutat. Res.* **211**, 279–289.

de Laat, W.L., Jaspers, N.G. and Hoeijmakers, J.H. (1999). Molecular mechanism of nucleotide excision repair. *Genes Dev.* **13**, 768–785.

Li, Y., Kuppusamy, P., Zweir, J. L. and Trush, M. A. (1996). Role of Cu/Zn-superoxide dismutase in xenobiotic activation. II. Biological effects resulting from the Cu/Zn-superoxide dismutase-accelerated oxidation of the benzene metabolite 1,4-hydroquinone. *Mol. Pharmacol.* **49**, 412–421.

Luo, L., Jiang, L., Geng, C., Cao, J. and Zhong, L. (2008). Hydroquinone-induced genotoxicity and oxidative DNA damage in HepG2 cells. *Chem. Biol. Interact.* **173**, 1–8.

Martone, T., Airoldi, L., Magagnotti, C., Coda, R., Randone, D., Malaveille, C., Avanzi, G., Merletti, F., Hautefeuille, A. and Vineis, P. (1998). 4-Aminobiphenyl-DNA adducts and p53 mutations in bladder cancer. *Int. J. Cancer* **75**, 512–516.

Mateos, R. and Bravo, L. (2007). Chromatographic and electrophoretic methods for the analysis of biomarkers of oxidative damage to macromolecules (DNA, lipids, and proteins). *J. Sep. Sci.* **30**, 175–191.

Mates, J. M., Segura, J. A., Alonso, F. J. and Marquez, J. (2008). Intracellular redox status and oxidative stress: Implications for cell proliferation, apoptosis, and carcinogenesis. *Arch. Toxicol.* **82**, 273–299.

Mates, J. M., Segura, J. A., Alonso, F. J. and Marquez, J. (2012). Oxidative stress in apoptosis and cancer: An update. *Arch. Toxi-*

col. **86**, 1649–1665.

Ma, H., Wang, J., Abdel-Rahman, S. Z., Boor, P. J. and Khan, M. F. (2008). Oxidative DNA damage and its repair in rat spleen following subchronic exposure to aniline. *Toxicol. Appl. Pharmacol.* **233**, 247–253.

Maynard, S., Schurman, S. H., Harboe, C., de Souza-Pinto, N. C. and Bohr, V. A. (2009). Base excision repair of oxidative DNA damage and association with cancer and aging. *Carcinogenesis* **30**, 2–10.

Micale, R. T., La Maestra, S., Di Pietro, A., Visalli, G., Baluce, B., Balansky, R., Steele, V. E. and De Flora, S. (2013). Oxidative stress in the lung of mice exposed to cigarette smoke either early in life or in adulthood. *Arch. Toxicol.* **87**, 915–918.

Moreno-Manzano, V., Ishikawa, Y., Lucio-Cazana, J. and Kitamura, M. (2000). Selective involvement of superoxide anion, but not downstream compounds hydrogen peroxide and peroxynitrite, in tumor necrosis factor-alpha-induced apoptosis of rat mesangial cells. *J. Biol. Chem.* **275**, 12684–12691.

Moslen, M. T. (1994). Reactive oxygen species in normal physiology, cell injury and phagocytosis. *Adv. Exp. Med. Biol.* **366**, 17–27.

Natoli, G., Costanzo, A., Ianni, A., Templeton, D. J., Woodgett, J. R., Balsano, C. and Levrero, M. (1997). Activation of SAPK/JNK by TNF receptor 1 through a noncytotoxic TRAF2-dependent pathway. *Science* **275**, 200–203.

Pagoria, D. and Geurtsen, W. (2005). The effect of N-acetyl-l-cysteine and ascorbic acid on visible-light-irradiated camphorquinone/N,N-dimethyl-p-toluidine-induced oxidative stress in two immortalized cell lines. *Biomaterials* **26**, 6136–6142.

Proctor, P. H.,2008) Uric acid: neuroprotective or neurotoxic? *Stroke*, **39**, e88–e89.

Richard, M.J., Portal, B., Meo, J., Coudray, C., Hadjian, A. and Favier, A. (1992). Malondialdehyde kit evaluated for determining plasma and lipoprotein fractions that react with thiobarbituric acid. *Clin. Chem.* **38**, 704–709.

Schreck, R., Rieber, P. and Baeuerle, P. A. (1991). Reactive oxygen intermediates as apparently widely used messengers in the activation of the NF-kappa B transcription factor and HIV-1. *EMBO J.* **10**, 2247–2258.

Setsukinai, K., Urano, Y., Kakinuma, K., Majima, H. J. and Nagano, T. (2003). Development of novel fluorescence probes that can reliably detect reactive oxygen species and distinguish specific species. *J. Biol. Chem.* **278**, 3170–3175.

Short, C. R., Joseph, M. and Hardy, M. L. (1989). Covalent binding of [14C]-2,6-dimethylaniline to DNA of rat liver and ethmoid turbinate. *J. Toxicol. Environ. Health* **27**, 85–94.

Skipper, P. L. (1996). Influence of tertiary structure on nucleophilic substitution reactions of proteins. *Chem. Res. Toxicol.* **9**, 918–923.

Skipper, P. L., Kim, M. Y., Sun, H. L., Wogan, G. N. and Tannenbaum, S. R. (2010). Monocyclic aromatic amines as potential human carcinogens: Old is new again. *Carcinogenesis* **31**, 50–58.

Skipper, P. L., Tannenbaum, S. R., Ross, R. K. and Yu, M. C. (2003). Nonsmoking-related arylamine exposure and bladder cancer risk. *Cancer Epidemiol. Biomarkers Prev.* **12**, 503–507.

Skipper, P. L., Trudel, L. J., Kensler, T. W., Groopman, J. D., Egner, P. A., Liberman, R. G., Wogan, G. N. and Tannenbaum, S. R. (2006). DNA adduct formation by 2,6-dimethyl-, 3,5-dimethyl-, and 3-ethylaniline in vivo in mice. *Chem. Res. Toxicol.* **19**, 1086–1090.

Stiborova, M., Miksanova, M., Havlicek, V., Schmeiser, H. H. and Frei, E. (2002). Mechanism of peroxidase-mediated oxidation of carcinogenic o-anisidine and its binding to DNA. *Mutat. Res.* **500**, 49–66.

Suzuki, Y. J., Forman, H. J. and Sevanian, A. (1997). Oxidants as stimulators of signal transduction. *Free Radic. Biol. Med.* **22**, 269–285.

Tao, L., Day, B. W., Hu, B., Xiang, Y. B., Wang, R., Stern, M. C., Gago-Dominguez, M., Cortessis, V. K., Conti, D. V., Van Den Berg, D., *et al.* (2013). Elevated 4-aminobiphenyl and 2,6-dimethylaniline hemoglobin adducts and increased risk of bladder cancer among lifelong nonsmokers—The Shanghai Bladder Cancer Study. *Cancer Epidemiol. Biomarkers Prev.* **22**, 937–945.

Thompson, L. H., Rubin, J. S., Cleaver, J. E., Whitmore, G. F. and Brookman, K. (1980). A screening method for isolating DNA repair-deficient mutants of CHO cells. *Somatic Cell Genet.* **6**, 391–405.

Tsuneoka, Y., Dalton, T. P., Miller, M. L., Clay, C. D., Shertzer, H. G., Talaska, G., Medvedovic, M. and Nebert, D. W. (2003). 4-aminobiphenyl-induced liver and urinary bladder DNA adduct formation in Cyp1a2(-/-) and Cyp1a2(+/+) mice. *J. Natl. Cancer Inst.* **95**, 1227–1237.

Ye, W., Seneviratne, U. I., Chao, M. W., Ravindra, K. C., Wogan, G. N., Tannenbaum, S. R. and Skipper, P. L. (2012). Transimination of quinone imines: A mechanism for embedding exogenous redox activity into the nucleosome. *Chem. Res. Toxicol.* **25**, 2627–2629.